Supporting information of "Material Design of Green-Light-Emitting Semiconductors: Perovskite-Type Sulfide $SrHfS_3$"

Kota Hanzawa,[1] Soshi Iimura,[1] Hidenori Hiramatsu,[1,2,*] and Hideo Hosono[1,2]

[1]Laboratory for Materials and Structures, Institute of Innovative Research, Tokyo Institute of Technology, Mailbox R3-3, 4259 Nagatsuta-cho, Midori-ku, Yokohama 226-8503, Japan

[2]Materials Research Center for Element Strategy, Tokyo Institute of Technology, Mailbox SE-1, 4259 Nagatsuta-cho, Midori-ku, Yokohama 226-8503, Japan

Correspondence and requests for materials should be addressed to H. Hiramatsu.

[*]H. Hiramatsu, e-mail: h-hirama@mces.titech.ac.jp

Text S1.

The *Pnma* superstructure has a √2 × √2 times larger *ac*-plane and 2 times longer *b*-axis compared with the $Pm\bar{3}m$ structure. The structural transformation in the *ac*-plane is illustrated in **Fig. S1**(a) and the corresponding reciprocal lattice folding is shown in (b). In real space, the primitive cubic lattice (black) has a lattice translation vector $\mathbf{T}_{2D} = u_1\boldsymbol{a} + u_3\boldsymbol{c}$, where $\boldsymbol{a}$ and $\boldsymbol{c}$ are primitive translation vectors, and u_1 and u_3 are integers. Through the change of the unit cell size (orange), each primitive translation vector rotates 45° in the *ac*-plane and becomes √2 times longer. As a result, the lattice translation vector changes to $\mathbf{T'}_{2D} = u'_1\boldsymbol{a'} + u'_3\boldsymbol{c'}$, where $\boldsymbol{a'} = \boldsymbol{a} + \boldsymbol{c}$, $\boldsymbol{c'} = -\boldsymbol{a} + \boldsymbol{c}$, and u'_1 and u'_3 are integers. In reciprocal space, the reciprocal lattice vector is denoted as $\mathbf{G}_{2D} = v_1\boldsymbol{x} + v_3\boldsymbol{z}$, where $\boldsymbol{x}$ and $\boldsymbol{z}$ are primitive reciprocal lattice vectors, and v_1 and v_3 are integers. Reflecting the unit cell size change in real space, each primitive reciprocal lattice vector also rotates 45° in the *ac*-plane and becomes 1/√2 times shorter (blue). This changes $\mathbf{G}_{2D}$ to $\mathbf{G'}_{2D} = v'_1\boldsymbol{x'} + v'_3\boldsymbol{z'}$, where $\boldsymbol{x'} = (\boldsymbol{x} + \boldsymbol{z})/2$, $\boldsymbol{z'} = (-\boldsymbol{x} + \boldsymbol{z})/2$, and v'_1 and v'_3 are integers. Because of the shortening of the reciprocal lattice vector, some bands are left outside the first BZ defined by the $\boldsymbol{x}$ and $\boldsymbol{z}$. Consequently, those bands have to be folded along the $\mathbf{G'}_{2D}$ to the first BZ defined by the $\boldsymbol{x'}$ and $\boldsymbol{z'}$, and the number of bands becomes double. This indicates that bands at the R point are folded to the Y point. This unit cell transformation in real space corresponds to structural transformation from $Pm\bar{3}m$ to *P*4/*mbm*.

Next, we consider the structural transformation to *Pnma* along the *b*-axis. In real space, the *b*-axis of *Pnma* is 2 times longer than before the structural transformation, as shown in (c, green). The lattice translation vector $\mathbf{T} = u'_1\boldsymbol{a'} + u_2\boldsymbol{b} + u'_3\boldsymbol{c'}$ changes to **T'**

$= u'_1\boldsymbol{a'} + u'_2\boldsymbol{b'} + u'_3\boldsymbol{c'}$, where $\boldsymbol{b}$ and $\boldsymbol{b'}$ are primitive lattice translation vectors before and after the structural transformation ($\boldsymbol{b'} = 2\boldsymbol{b}$), and u_2 and u'_2 are integers. The corresponding BZ size becomes half, as displayed in (d, red). The reciprocal lattice vector $\mathbf{G} = n'_1\boldsymbol{x'} + n_2\boldsymbol{y} + n'_3\boldsymbol{z'}$ changes to $\mathbf{G'} = n'_1\boldsymbol{x'} + n'_2\boldsymbol{y'} + n'_3\boldsymbol{z'}$, where $\boldsymbol{y}$ and $\boldsymbol{y'}$ are primitive lattice translation vectors before and after the structural transformation ($\boldsymbol{y'} = \boldsymbol{y}/2$), and n_2 and n'_2 are integers. This represents that bands at the Y point are folded to the Γ point through a translation operation in reciprocal space. In the inset in (e), BZ of $Pm\bar{3}m$ is shown. Here, blue and red arrows represent how the VBM at the R point transfers to the Γ point through the structural transformations in the *ac*-plane and along the *b*-axis. The resultant band folding is shown in (e). The VBM at the R point is folded first to the Y point, and finally to the Γ point.

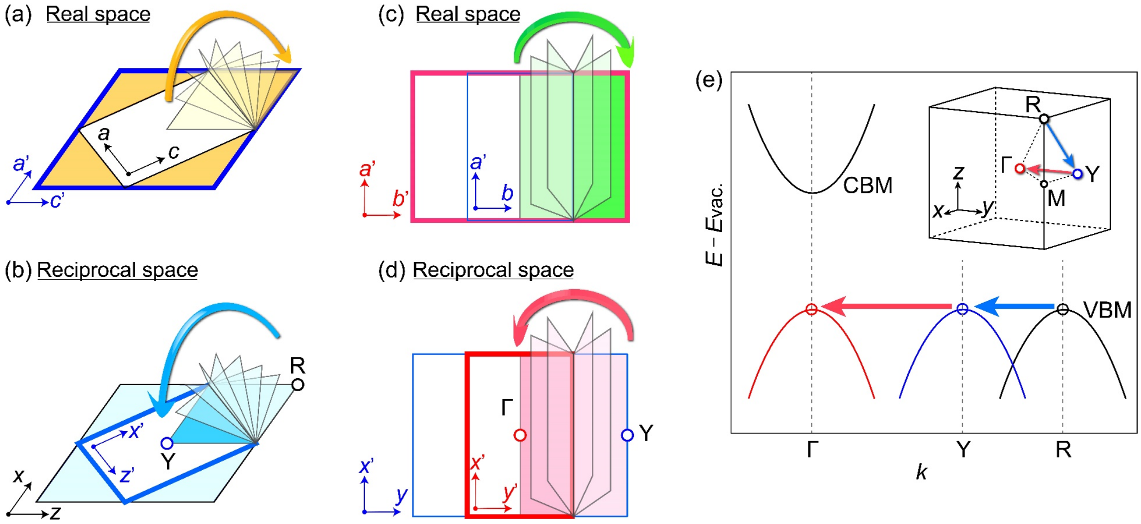

Figure S1. Band folding through structural transformation in perovskite from cubic $Pm\bar{3}m$ to orthorhombic *Pnma*.

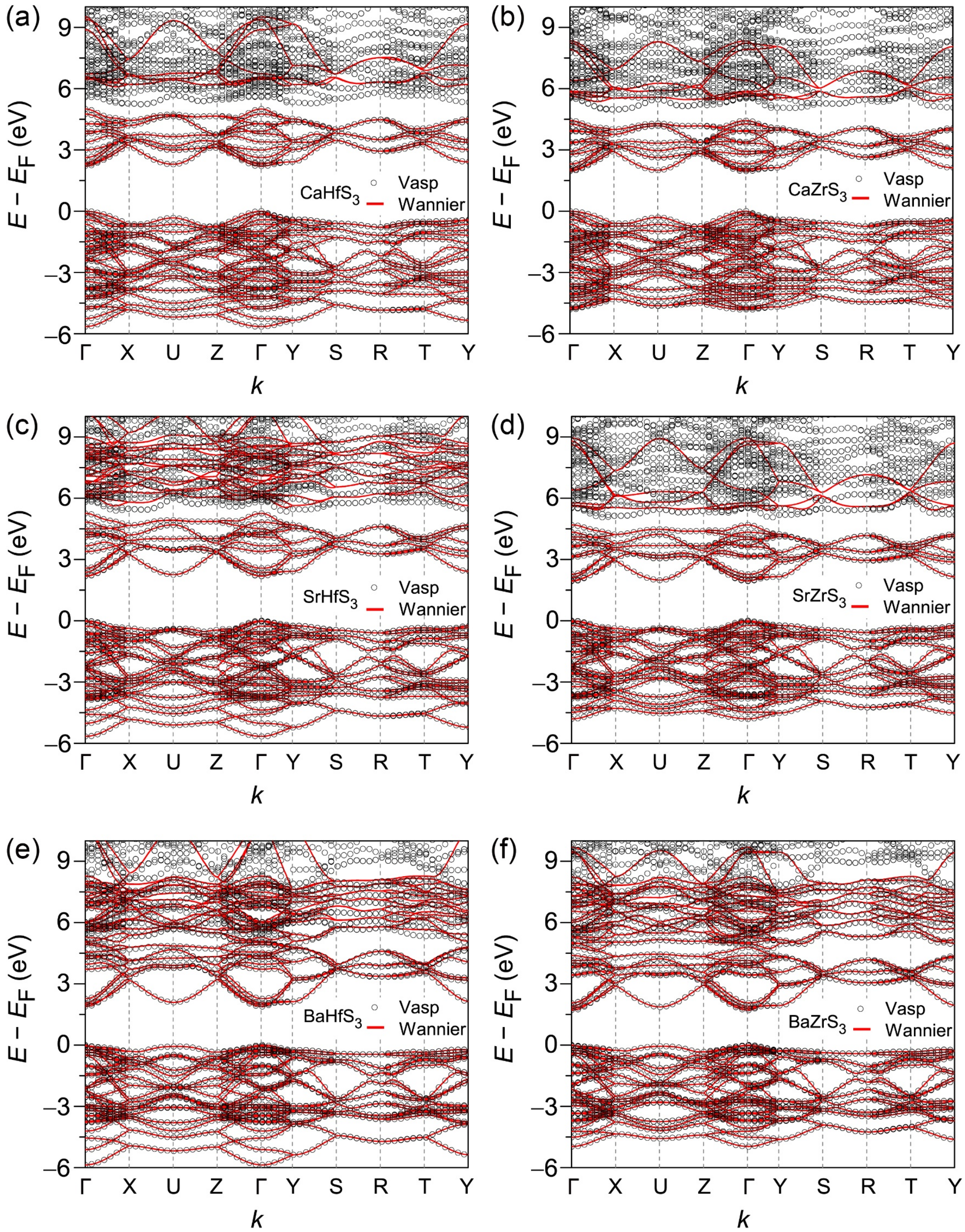

Figure S2. Band structures of *AE*-*eTM*-S$_3$. **S2a**, **S2c**, and **S2e** denote those of *AE*-HfS$_3$, where *AE* = Ca, Sr and Ba, respectively; whereas **S2b**, **S2d**, and **S2f** correspond to *AE*-ZrS$_3$ (*AE* = Ca, Sr, and Ba, respectively). Black circles are results of band structure calculations of *AE*-*eTM*-S$_3$ using VASP code, while red lines are computed using Wannier interpolation.

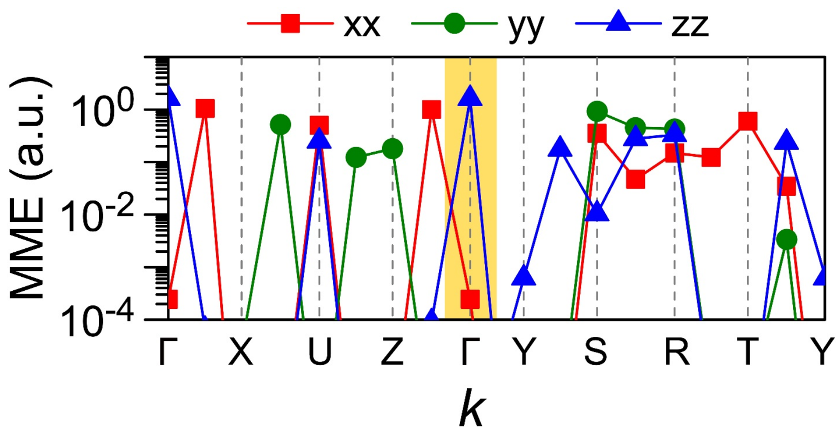

Figure S3. Calculated momentum matrix elements (MME) from the valence band edge to conduction band edge of $SrHfS_3$ at each *k* point.

Table S1. Calculated effective masses and band gaps of *AE*-*eTM*-S_3.

	m_e^* (m_0)			m_h^* (m_0)			E_g (eV)
	Γ–X	Γ–Y	Γ–Z	Γ–X	Γ–Y	Γ–Z	
$CaHfS_3$	0.30	0.51	0.46	0.78	0.18	0.62	2.21
$SrHfS_3$	0.40	0.26	0.43	0.70	0.19	0.61	2.18
$BaHfS_3$	0.31	0.19	0.39	0.19	0.69	0.56	1.90
$CaZrS_3$	0.31	0.60	0.48	0.85	0.18	0.61	1.95
$SrZrS_3$	0.41	0.26	0.44	0.75	0.19	0.61	1.94
$BaZrS_3$	0.33	0.20	0.41	0.19	0.70	0.52	1.72

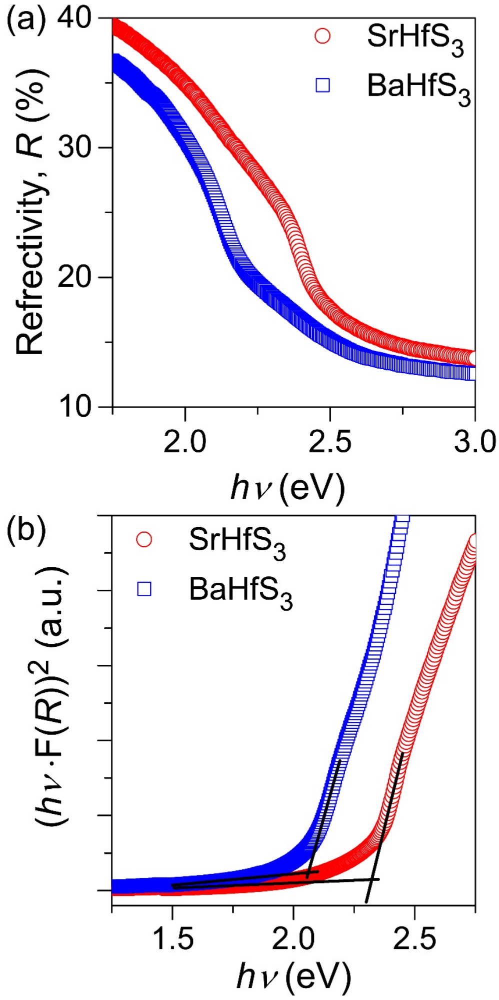

Figure S4. (a) Diffuse reflectance spectra and (b) the Kubelka–Munk plot of $SrHfS_3$ (red circles) and $BaHfS_3$ (blue squares). For the plot, we performed a transformation using the following equation; $F(R) = (1-R)^2/2R = K/S$, where K and S indicate optical absorption and scattering coefficients, respectively. Linear lines in (b) are results of the least-squares fittings.

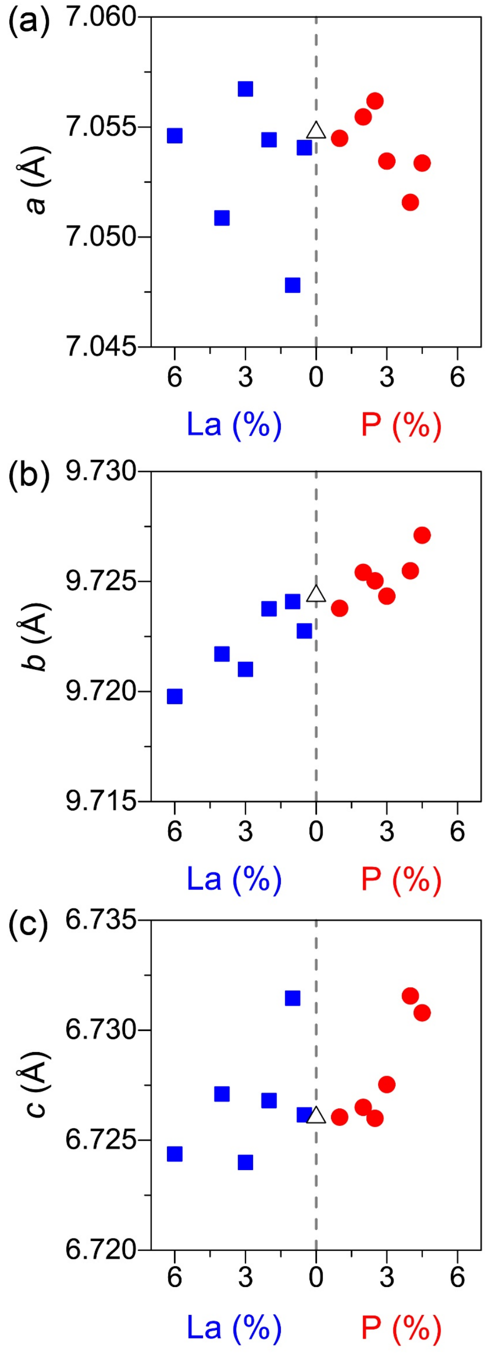

Figure S5. (a) *a*-, (b) *b*- and (c) *c*-axes lattice parameter variations in $SrHfS_3$ through La- (blue squares) and P-dopings (red circles). The horizontal axis denotes nominal La- and P-doping concentrations.

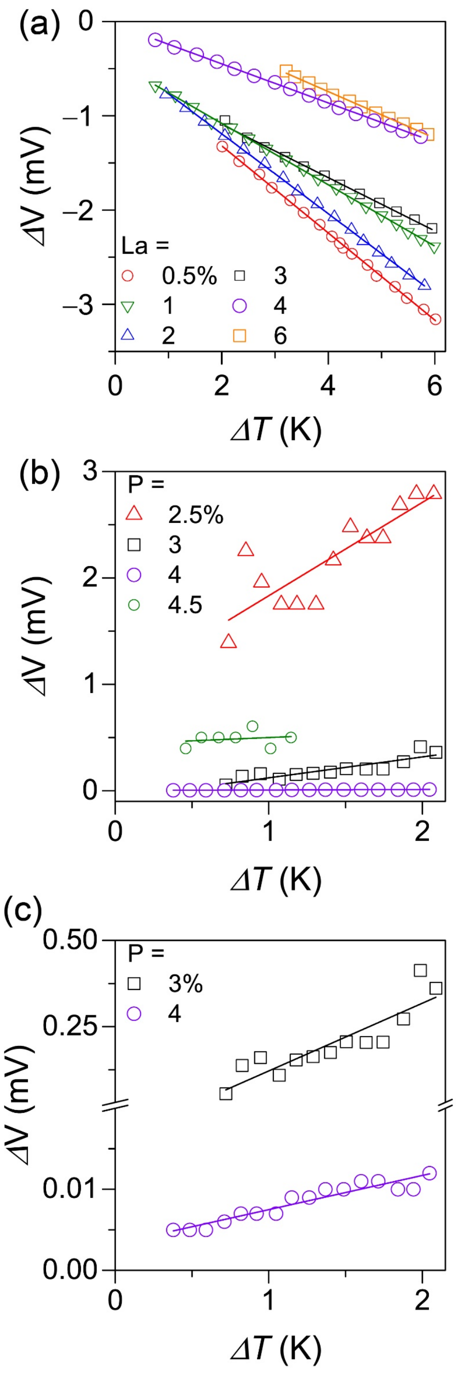

Figure S6. Thermopower measurement of (a) La- and (b) P-doped $SrHfS_3$ as a function of nominal doping concentrations. (c) The enlarged plots for the 3% and 4% P-doped samples shown in (b). The least-squares fitting results are delineated as straight lines.

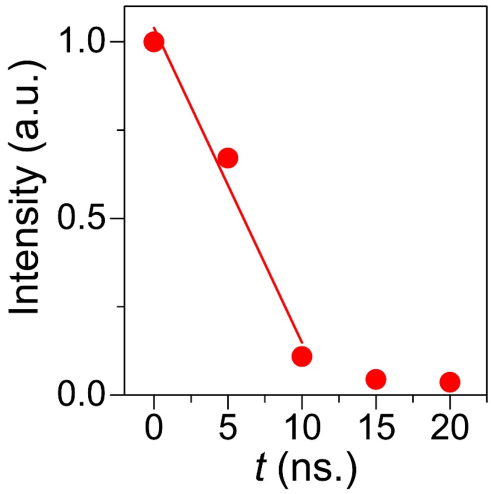

Figure S7. Decay curve of undoped $SrHfS_3$ at 30 K. Red line is a result of the least-squares fitting for the single-decay model emission lifetime.

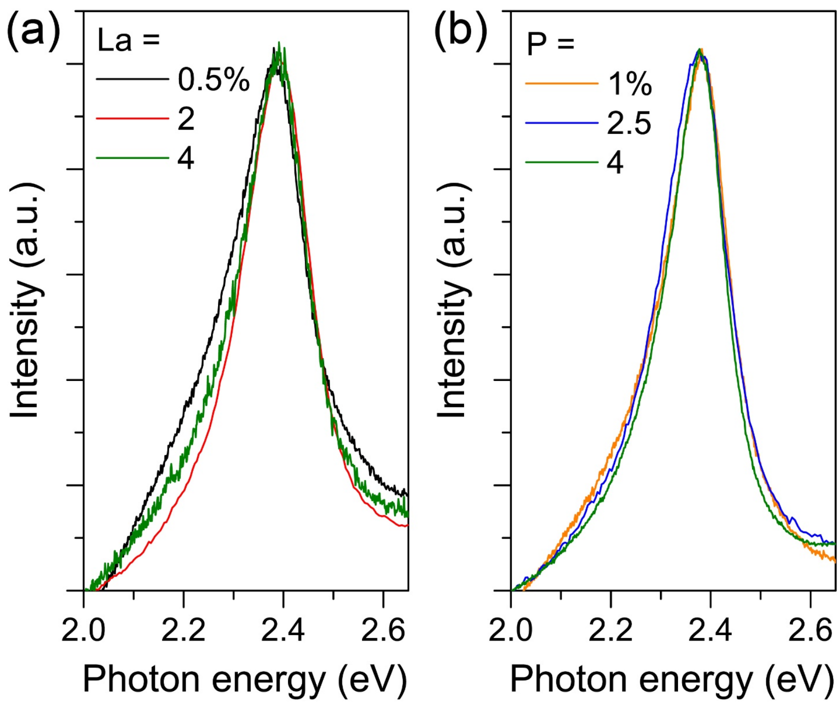

Figure S8. Photoluminescence (PL) spectra of (a) La- and (b) P-doped $SrHfS_3$ taken at 300 K. Black, red, and green lines in (a) correspond to PL spectra at La-doping concentrations of 0.5%, 2%, and 4%, respectively. Orange, blue, and green lines denote PL spectra of 1%, 2.5%, and 4% P-doped $SrHfS_3$.